

Assessing the Thickness of Thin Films Based on Elemental Data Composition of Film Structures

Yu. M. Nikolaenko^{a*}, A. S. Korneevets^a, N. B. Efros^a,
V. V. Burkhovetskii^a, and I. Yu. Reshidova^a

^a O.O. Galkin Donetsk Institute for Physics and Engineering, 83114 Donetsk, Ukraine

*e-mail: nik@donfti.ru

Received February 21, 2019; revised April 8, 2019; accepted April 11, 2019

Abstract—We demonstrate the possibility of a quantitative assessment of the thickness of thin films using to measurements of the cationic composition of film structures using the INCA Energy-350 energy dispersion spectrometer that is part of the JSM-6490 LV electron microscope (Japan). The use of this method is especially useful if it is impossible to provide sufficient contrast between the images of the film and substrate sections obtained with a scanning electron microscope on a transverse cleavage of the film structure.

Keywords: scanning electron microscope, energy dispersive X-ray spectrometer, nanosized films, magnetron sputtering method of targets.

DOI: 10.1134/S1063785019070083

Film thickness is a key parameter for quantitative characterization of many physical processes that provide the functioning of modern technical devices. This concerns electron and diffusion transport, as well as optical, thermal and magnetic phenomena. In addition, in certain techniques, the maintenance of optimum thickness is a prerequisite for ensuring the functional quality of thin metal coatings [1]. Electron microscopes are often used to control the thickness of thin films, and methods of measurement change depending on the specific problem. The most common method to estimate the thickness of the transverse cleavage of a film structure is the use of the image obtained with a scanning electron microscope (SEM) [1–5]. At the same time, not all existing methods can be successfully applied under certain conditions. In some cases, to obtain reliable information, researchers are forced to use several alternative methods [6] and search for new opportunities. Examples of the development of original methods for controlling the thickness of ultrathin films [7] and film layers of biological objects [8] are known. In this paper, we propose a new indirect method for estimating the film thickness based on the standard capabilities of the electron microscope.

The INCA Energy-350 LV energy dispersive spectrometer (JEOL, Japan) [9] is widely used for studies of an elemental composition in various samples of multicomponent chemical compounds. The principle of operation of this spectrometer principle is dispersion analysis of the characteristic X-ray radiation from the surface layer region of the sample irradiated by an

electron beam. A digital report on the elemental composition of the chemical compound in the studied area is formed from the measurement results. The area with an excited state of matter has a microscopic size from 1–5 to 10 μm in depth from the surface. In particular, this enables obtaining information on the homogeneity of chemical compound composition in various local regions of the near-surface layer of the sample.

In the case of film structures that have the form of a nanothick film on a relatively thick substrate, the spectrometer gives the information about the film and substrate elemental composition. In the digital report of the spectrometer, the total content of atoms is normalized to 100%. As a result, when measuring the composition in the film structures with the films of different thickness, the ratio between the film and substrate atomic concentrations changes. This is something that we noted earlier [10]. In this paper, based on the data of energy dispersive analysis, we explored the possibility of indirect film thickness control.

For this purpose, a series of film structures with different film deposition time was fabricated. The films were fabricated by the method of magnetron sputtering of a $\text{La}_{0.7}\text{Sr}_{0.3}\text{MnO}_{3-\delta}$ (LSMO) ceramic target on single-crystal NdGaO_3 substrates. The substrate material was chosen so that the cationic composition of the film and substrate materials was different, but their crystalline parameters had a small mismatch [11]. The latter is necessary to provide conditions of epitaxial film growth [12–14].

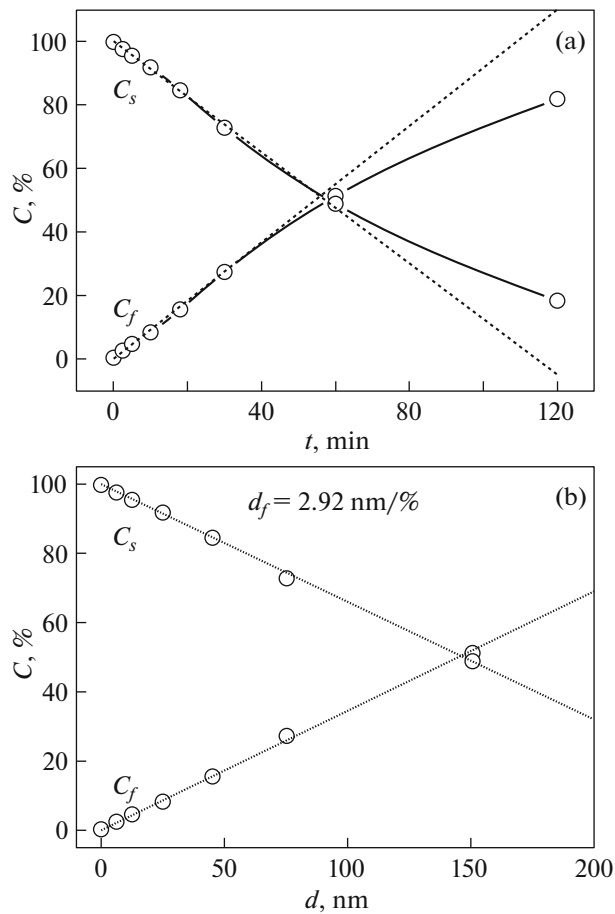


Fig. 1. Variation of the relative cationic composition of the film and the substrate, depending on (a) the duration of an epitaxial growth of LSMO films and (b) film thickness.

Figure 1a shows the result of measuring the total cationic composition of materials of the film (C_f) and the substrate (C_s) using the energy dispersive spectrometer. Since LSMO films produced in accordance with our technique are oxygen-deficient [15, 16], the oxygen content was excluded from the calculations. Therefore, the total cation concentration is normalized to 100%: $C_f + C_s = 100\%$, where $C_f = C(\text{La}) + C(\text{Sr}) + C(\text{Mn})$ and $C_s = C(\text{Nd}) + C(\text{Ga})$. As can be seen from Fig. 1a, the cation concentration monotonously increases with increasing the film growth time, while the concentration of cations in the substrate, respectively, decreases. In addition, a significant part of dependence $C_f(t)$ is well approximated by a linear function.

Figure 2 shows the thickness of the part of the films having a relatively large growth time estimated using a gravimetric method. Gravimetric measurements of film structures were carried out using a balance with an Ohaus Analytical Plus digital display (Switzerland), which allows one to control five signs with a minimum value of 10^{-5} g. The film area was about 0.4 cm^2 . To

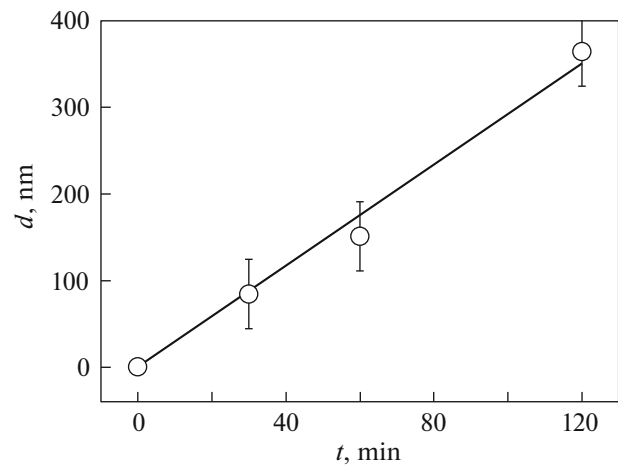


Fig. 2. Assessment of the thickness of LSMO films based on gravimetric method data.

avoid deposition of the film material on the side surfaces of the substrate, the growth of films was carried out using a metal mask with a rectangular window. Otherwise, a noticeable error is possible that leads to a decrease in the calculated thickness [10].

It should be noted that the thickness estimated by the gravimetric method gives some average value (without taking into account its change from the central to the peripheral part of the film). At the same time, the uniformity of thickness of films with a size of $1 \times 1 \text{ cm}$, in accordance with the previous assessment, holds with an accuracy of no worse than 5–10% [15]. Taking into account that the result of measuring the film thickness by the gravimetric method has a low accuracy (Fig. 2), it is necessary to accept the fact that the film thickness increases linearly with the time of their deposition. At least, it is not possible to clarify this dependence using our data. Thus, it is possible to convert the data on the change in the relative cationic composition of the film and the substrate, depending on the duration of their growth (see Fig. 1a), into dependence $C(d)$ (Fig. 1b).

Dependence $C_f(d)$ in Fig. 1b is plotted in that part where it can be represented by a linear function, without data corresponding to the maximum film deposition time of 120 min. Already at a film thickness of 150 nm, the film and substrate cation concentrations become approximately equal. For larger film thicknesses, nonlinearity is revealed, which may be caused by the film effect on the measured cation composition of the substrate. In the linear region, the dependence of the relative cation concentration of the film on its thickness is characterized by a coefficient of approximately $2.9 \text{ nm}/\%$.

Thereafter, with this tool to control film thickness in hand, we investigated the change in the sputtering rate of the target after its restoration. After long-term use, the target acquires a relief in form with a signifi-

cant loss of material in an annular region with a diameter of 16–32 mm. An additional layer is formed, which is a number of sputtering oxide products of the material, in the central part of the target with a diameter of less than 16 mm. To eliminate the relief of the target, we use mechanical grinding of its surface.

It is known that new well-sintered ceramic targets exhibit a reduced sputtering rate of material at the beginning of operation. As we found out earlier, the sputtering rate increases sequentially and stabilizes within a few hours during the use of the target. Apparently, this is due to the process of defect formation in crystallites located in the surface layer of the target. If this effect is really associated only with a thin surface layer, then the sputtering rate should change in a similar way after relief removal in the restored target. To obtain quantitative characteristics after eliminating the target topography, we fabricated a series of LSMO/Al₂O₃ film structures with the same exposure time (1 h). The substrate material was chosen by economical reasons. The cationic compositions for a series of films and substrates do not match, which allows us to determine them separately, but the crystalline structures are different. For this reason, the films have a polycrystalline microstructure. Figure 3a shows the measurement results.

As can be seen from Fig. 3a, the relative cationic concentration of the film is described by the dependence with saturation. Accordingly, the dependence averaged for a time of 1 h of the target sputtering rate (Fig. 3b) also shows a gradual growth and stabilizes within 6–7 h. Thus, we obtained the expected result. After removing a thin surface layer from the surface of the target, its sputtering rate is similar to the sputtering rate of a new target. This, in turn, confirms our hypothesis that the mechanism of sputtering rate formation is associated with defect formation in microscopic crystallites located in the near-surface layer of the target.

It should be noted that the most accessible indirect method for evaluating the film thickness by exposure time is not always successful. For some functional materials, the manufacture of targets with a sufficiently strong mechanical coupling of crystallites is a technological problem. An example is indium oxide. Target samples based on both pure and strontium-doped indium oxides demonstrate an unstable sputtering rate due to insufficient mechanical strength.

In conclusion, we note the practical significance of the proposed methods for estimating the thickness of films. First, it is not expensive, since cationic composition control using SEM is a regular operation and allows one to study a series of film structures in a relatively short time. Second, the proposed method is nondestructive. An alternative method of film thickness control when use is made of the SEM images of the butt end of the film structure involves additional machining, for example, the manufacture of a trans-

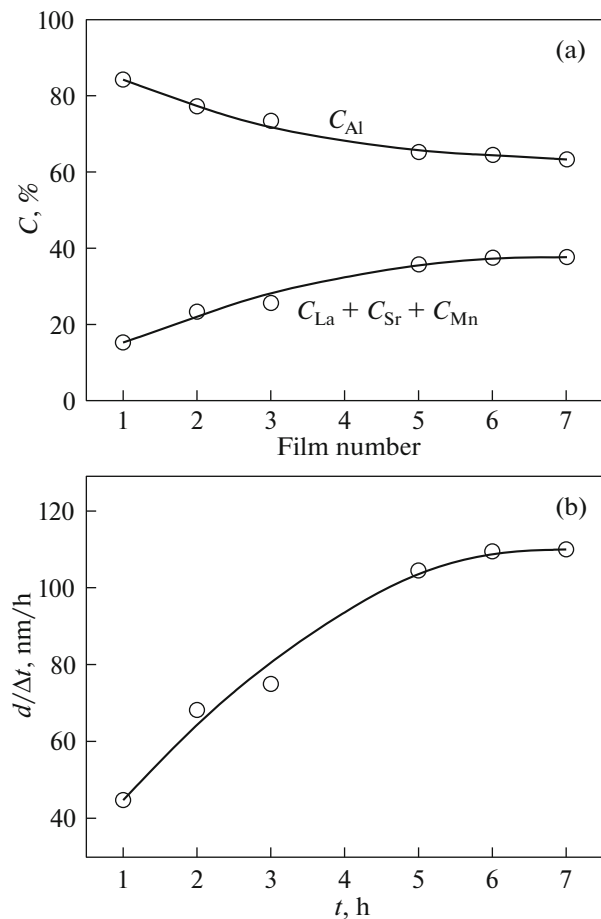


Fig. 3. (a) Variation of the relative cationic composition of the film and substrate materials depending on the sequence of deposition of films (exposure time 1 h); (b) variation of the film growth rate depending on the sputtering time of the target after its mechanical polishing.

verse cleavage. In addition, obtaining sufficient contrast between the images of the film and the substrate is often a problem. In the case of LSMO/SrTiO₃ film structures, when the film material contains much heavier atoms than the substrate material, this problem is less expressed. But the image contrast in the image of the transverse cleavage of the LSMO/NdGaO₃ film structure mainly characterizes the relief of a cleaved surface. As a result, determining the film–substrate interface position for an SEM image becomes extremely problematic [17].

CONFLICT OF INTEREST

The authors declare that they have no conflict of interest.

REFERENCES

1. R. V. Selyukov, V. V. Naumov, and S. V. Vasilev, *Tech. Phys.* **63**, 900 (2018).

2. M. Yu. Presnyakov, B. V. Sladkoptsev, and E. K. Belonogov, *Tech. Phys. Lett.* **42**, 1149 (2016).
3. A. R. Shugurov, A. A. Akulinkin, A. M. Kasterov, and M. P. Kalashnikov, *Tech. Phys. Lett.* **45** (2019, in press).
4. R. G. Valeev, D. I. Petukhov, A. I. Chukavin, and A. N. Bel'tyukov, *Tech. Phys. Lett.* **42**, 124 (2016).
5. M. A. Mussaeva and E. M. Ibragimova, *Tech. Phys. Lett.* **45**, 155 (2019).
6. G. I. Kotov, S. V. Kuzubov, B. L. Agapov, G. A. Panin, and N. N. Bezryadin, *Kondens. Sredy Mezhfaz. Granitsy* **14**, 429 (2012).
7. S. Yu. Kupreenko, N. A. Orlikovskii, E. I. Rau, A. M. Tagachenkov, and A. A. Tagachenkov, *Tech. Phys.* **60**, 1515 (2015).
8. A. A. Adamov and V. N. Khramov, *Mat. Fiz. Komp'yut. Model.* **20** (4), 83 (2017).
9. www.jeol.co.jp/en.
10. Yu. M. Nikolaenko, V. V. Burkhovetskii, A. S. Korneevets, N. B. Efros, I. Yu. Reshidova, A. A. Tikhii, I. V. Zhikharev, and V. V. Faraponov, *Fiz. Tekh. Vys. Davl.* **27** (4), 116 (2017).
11. G. A. Ovsyannikov, A. M. Petrzhik, I. V. Borisenko, A. A. Klimov, Yu. A. Ignatov, V. V. Demin, and S. A. Nikitov, *J. Exp. Theor. Phys.* **108**, 48 (2009).
12. V. I. Belyavskii, *Soros. Obrazov. Zh.*, No. 10, 92 (1998).
13. Yu. M. Nikolaenko, A. B. Mukhin, V. A. Chaika, and V. V. Burkhovetskii, *Tech. Phys.* **55**, 1189 (2010).
14. I. V. Borisenko, V. V. Demidov, A. A. Klimov, G. A. Ovsyannikov, K. I. Konstantinyan, S. A. Nikitov, V. L. Preobrazhenskii, N. Tiercelin, and P. Pernod, *Tech. Phys. Lett.* **42**, 113 (2016).
15. V. N. Varyukhin, Yu. M. Nikolaenko, Yu. V. Medvedev, A. B. Mukhin, B. V. Belyaev, V. A. Gritskikh, I. V. Zhikharev, S. V. Murza, N. V. Korchikova, and A. A. Tikhii, *Tech. Phys. Lett.* **35**, 937 (2009).
16. Yu. M. Nikolaenko, A. N. Artemov, Yu. V. Medvedev, N. B. Efros, I. V. Zhikharev, I. Yu. Reshidova, A. A. Tikhii, and S. V. Kara-Murza, *J. Phys. D: Appl. Phys.* **49**, 375302 (2016).
17. Yu. M. Nikolaenko, V. V. Burkhovetskii, A. S. Korneevets, N. B. Efros, and I. Yu. Reshidova, *Fiz. Tekh. Vys. Davl.* **28** (4), 78 (2018).

Translated by G. Dedkov